4878–4892 *Nucleic Acids Research, 2006, Vol. 34, No. 17* *Published online 14 September 2006*
doi:10.1093/nar/gkl651

Isolation and characterization of the *TIGA* genes, whose transcripts are induced by growth arrest

Norikazu Yabuta[1], Hiroaki Onda[1], Masafumi Watanabe[1,2], Naohisa Yoshioka[1], Ippei Nagamori[1], Tomoyuki Funatsu[1], Shingo Toji[2], Katsuyuki Tamai[2] and Hiroshi Nojima[1,*]

[1]Research Institute for Microbial Diseases, Osaka University, 3-1 Yamadaoka, Suita, Osaka 567-0871, Japan and [2]Ina Laboratory, MBL Co. Ltd., 1063-103 Ohara, Terasawaoka, Ina, Nagano 396-0002, Japan

Received May 19, 2006; Revised August 12, 2006; Accepted August 24, 2006

ABSTRACT

We report here the isolation of 44 genes that are upregulated after serum starvation and/or contact inhibition. These genes have been termed *TIGA*, after Transcript Induced by Growth Arrest. We found that there are two kinds of G0 phases caused by serum starvation, namely, the shallow G0 (or G0/G1) and the deep G0 phases. The shallow G0 is induced by only a few hours of serum starvation, while deep G0 is generated after 3 days of serum starvation. We propose that mammalian cells enter deep G0 through a G0 gate, which is only opened on the third day of serum starvation. *TIGA1*, one of the uncharacterized *TIGA* genes, encodes a homolog of cyanate permease of bacteria and localizes in mitochondria. This suggests that Tiga1 is involved in the inorganic ion transport and metabolism needed to maintain the deep G0 phase. Ectopic expression of *TIGA1* inhibited not only tumor cell proliferation but also anchorage-independent growth of cancer cell lines. A microsatellite marker, *ENDL-1*, allowed us to detect loss of heterozygosity around the *TIGA1* gene region (5q21–22). Further analysis of the *TIGA* genes we have identified here may help us to better understand the mechanisms that regulate the G0 phase.

INTRODUCTION

Most of the cells in adult eukaryotic organisms do not divide. Instead, they remain in a state called the quiescent state or G0 phase in which macromolecular synthesis is largely reduced. There are at least three distinct conditions that induce eukaryotic cells to enter this quiescent state, namely, serum starvation, contact inhibition and terminal differentiation. We distinguish here between the states that are induced by these conditions by referring to them as G0-s, G0-c and G0-t, respectively. It is likely that the mechanisms that regulate these states share some similarities but diverge in other aspects. Normal somatic cells require the presence of mitogens for continual proliferation; upon the removal of such mitogens or upon contact inhibition, they exit the vegetative cell cycle at early/mid G1 phase and proceed to the G0 phase. In contrast, cancer cells are destined to repeat the cell cycle indefinitely and cannot be induced to enter the G0 phase by either serum starvation or contact inhibition.

Defining the G0 phase is hampered by difficulties in distinguishing it from the G1 phase. Consequently, the arrest point is sometimes referred to as G0/G1. More than a quarter of a century ago, the arrest point was first described as a restriction point that regulates cell growth and the division cycle (1). Zetterberg and Larsson (2) proposed that this restriction point divides the G1 phase into two parts; cells before this point can leave the cell division cycle and enter the G0 phase, while cells past this point are unaffected by a short period of serum deprivation. However, on the basis of his continuum model, Cooper (3) argued that a restrictive control point does not exist. Thus, not only are there no defined physiological or molecular markers that can be used to distinguish between the G0-s, G0-c and G0-t phases, the general nature of the G0 phase itself is poorly defined.

It has been revealed that the transition from G0 to G1 (G0/G1) is regulated in an analogous fashion to S phase entry, as it involves the inactivation of the retinoblastoma (Rb) protein by phosphorylation. Evidence for this is that acute somatic inactivation of Rb is sufficient to induce G0-arrested cells to re-enter the cell cycle (4). Moreover, the acute loss of Rb expression in primary quiescent cells due to an Rb mutation is also sufficient to induce their entry into the cell cycle entry (5). However, a different cyclin/cdk combination to the one involved in S phase entry mediates the Rb inactivation event in the G0/G1 transition, as it has been shown that cyclin C combines with Cdk3 during the G0/G1 transition and that this leads to the phosphorylation of Rb and the efficient exit of these cells from G0 (4). Moreover, it has been found that

*To whom correspondence should be addressed. Tel: +81 6 6875 3980; Fax: +81 6 6875 5192; Email: snj-0212@biken.osaka-u.ac.jp
Present address:
Naohisa Yoshioka, Howard Hughes Medical Institute, Department of Cellular and Molecular Medicine, UCSD School Medicine, 9500 Gilman Drive, La Jolla, CA 92093-0686, USA

the E3 complex KPC (Kip1 ubiquitination-promoting complex) plays a role in releasing the cells from G0 to G1 by degrading the cyclin-dependent kinase inhibitor p27 (Kip1) (6). Notably, E2F-6, which can silence genes in an Rb-independent manner, may also be involved in gene silencing in the G0 phase, as a multimeric E2F-6 complex that contains chromatin modifiers and Myc/Brachyury-binding regulators has been found to preferentially occupy target promoters in G0 cells rather than in G1 cells. This suggests that this complex participates in the silencing of the E2F- and Myc-responsive genes in quiescent cells (7).

It has been proposed that important regulatory factors are expressed in a G0 phase-specific manner to initiate and maintain the quiescent state. However, only a few studies have succeeded in isolating such genes or factors. In one such study, six growth-arrest-specific (gas) genes were isolated from serum-starved mouse cells (8). Of these genes, Gas1 was found to function during development as an inhibitor of growth and a mediator of cell death (9). Gas2 is an inhibitor of calpain, as it controls its transcript levels (10). However, determining the function of these gas genes has shed only limited light on the G0 phase, partly because so many of the genes that characterize the G0 phase have not yet been isolated and identified. Moreover, since the studies characterizing the gas genes focused on genes expressed in G0-s, the genes regulating G0-c and G0-t have not yet been explored.

To examine these issues further, we here report the isolation of novel genes that are upregulated after serum starvation and contact inhibition. We selected the putative G0-specific genes that are upregulated by serum starvation but not by contact inhibition for further characterization. We propose here that there are two kinds of G0 phases caused by serum starvation, namely, the shallow G0 (or G0/G1) and the deep G0 phases, and that there exists an entry point (the G0 gate) that is opened after 3 days of serum starvation. We show here that the shallow G0 is induced by a few hours of serum starvation, while the deep G0 phase is generated after 3 days of serum starvation.

MATERIALS AND METHODS

Cell lines and culture conditions

The normal human diploid fibroblast line TIG-1 was grown in DMEM supplemented with 10% FBS. For serum starvation, subconfluent cells were cultured for 96 h in DMEM containing 0.5% FBS. The six SCLC cell lines Lu-24, Lu-130, Lu-134-A, Lu-135, Lu-139, Lu-140 and H69; the six NSCLC cell lines A549, EBC-1, Lu-65, HEL, Jurkat and Raji are gifts from RIKEN Cell bank (Tokyo, Japan). PC-3, PC-7 and PC-10 cells are gifts from Dr T. Kohno (National Cancer Center Research Institute, Tokyo, Japan). These cell lines were grown in RPMI1640 medium supplemented with 10% FBS. The other cell lines, MRC-5, HeLa S3, MCF-7, Saos-2, T24 and EcR-293, were maintained in DMEM supplemented with 10% FBS.

Virus infection and soft agar assay

pCXbsr-HA-Tiga1 was constructed by ligating the EcoRI–NotI fragments of HA-tagged TIGA1 from pcDNA3-HA-TIGA1 into the EcoRI and NotI sites of pCXbsr, a Moloney murine leukemia virus (MuLV)-based retrovirus vector containing the blasticidin S resistance gene (bsr) as a selectable marker (11). Production of amphotropic retroviruses, virus infection of cancer cells and the soft agar assay were performed as previously described (11,12). Briefly, BOSC23 cells were co-transfected with pCXbsr-HA-Tiga1 and pCL-Ampho vector and incubated for 48 h. The culture supernatants were collected as amphotropic viral stocks. For virus infection, growing Saos-2 and T24 cells were treated with 8 μg/ml polybrene for 30 min and then incubated with the amphotropic retrovirus for 1 h at 37°C. After the blasticidin S (10 μg/ml) selection, cells were pooled and used for the experiments. For the soft agar assay, 10 000 growing cells were inoculated into 0.4% Noble agar containing DMEM supplemented with 10% FBS in a 60 mm dish. After 10 days of incubation, the number of colonies (>0.15 mm in diameter) in each plate was scored.

Preparation and expression of a fluorescent fusion protein of Tiga1

To prepare a plasmid construct that can express Tiga1 protein fused with enhanced green fluorescent protein (GFP), we first produced a DNA fragment carrying the entire ORF of Tiga1 by PCR using *TIGA1* cDNA as a template. To obtain the cDNA insert for Tiga1 carrying in-frame AscI–NotI sites, primers hybridizing to *TIGA1* around the initiation codon (5′-AGAATCCGGCGCGCCGATGGTACAGCCCGCT-3′; the AscI site is underlined) and the termination codon (5′-ATACTCGAGGCGGCCGCTCAGTTATACGGTAAGGC-3′; the NotI site is underlined) were synthesized and used in PCR. The resulting sequence was confirmed to be the *TIGA1* gene by sequencing the DNAs of three independent clones. The plasmid DNA without any mismatches was selected. Next, we incorporated the AscI/NotI-digested fragment of *TIGA1* into the pEGFP3B vector. COS-7 cells were transfected with the plasmid DNA harboring *EGFP-TIGA1* or the vector alone by using lipofectamine reagents (Invitrogen, San Diego, CA) according to the manufacturer's protocol and cultured in a 60 mm culture dishes at 37°C in a CO_2 incubator for 48 h, and were fixed as described previously (13,14). Photo images were recorded under a fluorescence microscope (Olympus, IX51).

Western blot analysis and protease protection assay

The transfection of plasmids into HeLa or MCF-7 cells, Western blot analysis and immune fluorescence analysis were performed as described previously (13). For western blot analysis, the proteins of the transfected cells were extracted in RIPA buffer after being washed with PBS(−), followed by electrophoretic separation and probing with antibodies against GFP (J1, a gift from Dr S. Fujita, Mistubishi Kasei, Tokyo, Japan), tubulin (Sigma, Milwaukee, WI), cytochrome c (Promega, Madison, WI) and Myc (PL14; MBL, Ina, Japan). Chloromethyl-X-rosamine (MitoTracker Red) was purchased from Molecular Probes Inc. (Eugene, OR). The protease protection assay was performed as described previously (13). Briefly, cells extracts from 6Myc-Tiga1-expressing HeLa cells were digested by various amounts of trypsin in the presence or absence of 1% Triton X-100 for

15 min. 6Myc-Tiga1 construct was prepared in a similar way as described previously (14). The trypsin digestion was rapidly inhibited by adding sample buffer and boiling. The boiled extracts were probed by western blot analysis using anti-Myc antibody.

RESULTS

Isolation of human TIGA genes

To isolate the human genes whose expression is upregulated in growth-arrested human embryo fibroblast TIG-1 cells, we first plated TIG-1 cells in DMEM supplemented with 10% FCS and then reduced the FCS concentration to 0.5% when they were in a semi-confluent state. The cells were cultured for 1–6 days in these serum-starved conditions and equal numbers were harvested daily and subjected to mRNA extraction. The daily mRNAs were used for time-course northern blot analysis and pooled to construct a cDNA library with the pAP3neo vector (15) (see Supplementary Data). Northern blot analysis using the *MCM2-7* genes as probes and the mRNAs obtained from the cells at 0–6 days after serum starvation was performed to confirm that the serum-starved cell population had actually entered the G0 phase of the cell cycle. We showed previously that the *MCM2-7* genes, which play pivotal roles in initiating the S phase of the cell cycle, are dramatically upregulated at the G1/S transition after being induced by the addition of serum to exit the G0 phase (16). Indeed, three days after serum deprivation, the *MCM2-7* mRNA levels in TIG-1 cells were markedly reduced (Figure 1A). Thus, the serum deprivation induced the cell population to enter a quiescent state.

We subjected the cDNA library constructed from these quiescent cells to the stepwise subtraction method we developed previously (17). In this process, we subtracted the cDNA clones that hybridized with the biotin-labeled mRNA obtained from exponentially growing TIG-1 cells by biotin–avidin interaction. This subtractive process was repeated four times in a stepwise manner. The genes that showed conspicuously stronger band intensities after serum starvation compared to the exponentially growing state (Log) in northern blot analysis were selected as potential growth-arrest-specific genes (data not shown). As a result, after the fourth stepwise subtraction, we isolated 44 cDNA clones that showed increased expression in the TIG-1 cells after serum starvation. These genes were collectively named *TIGA* after Transcript Induced by Growth Arrest (Table 1).

Time-course of *TIGA* mRNA expression after serum starvation and contact inhibition

To examine when during the process of entry into G0 phase each of the 44 *TIGA* genes become transcribed, we performed time-course northern blot analysis using the RNA extracted daily from TIG-1 cells over the six days of serum starvation (Figure 1B and C; Supplementary Figure S1B, left panels). We also examined whether these *TIGA* genes are induced by cell-cell contact, which inhibits cell proliferation (Figure 1B and C; Supplementary Figure S1, right panels). This was because the growth arrests that arise from contact

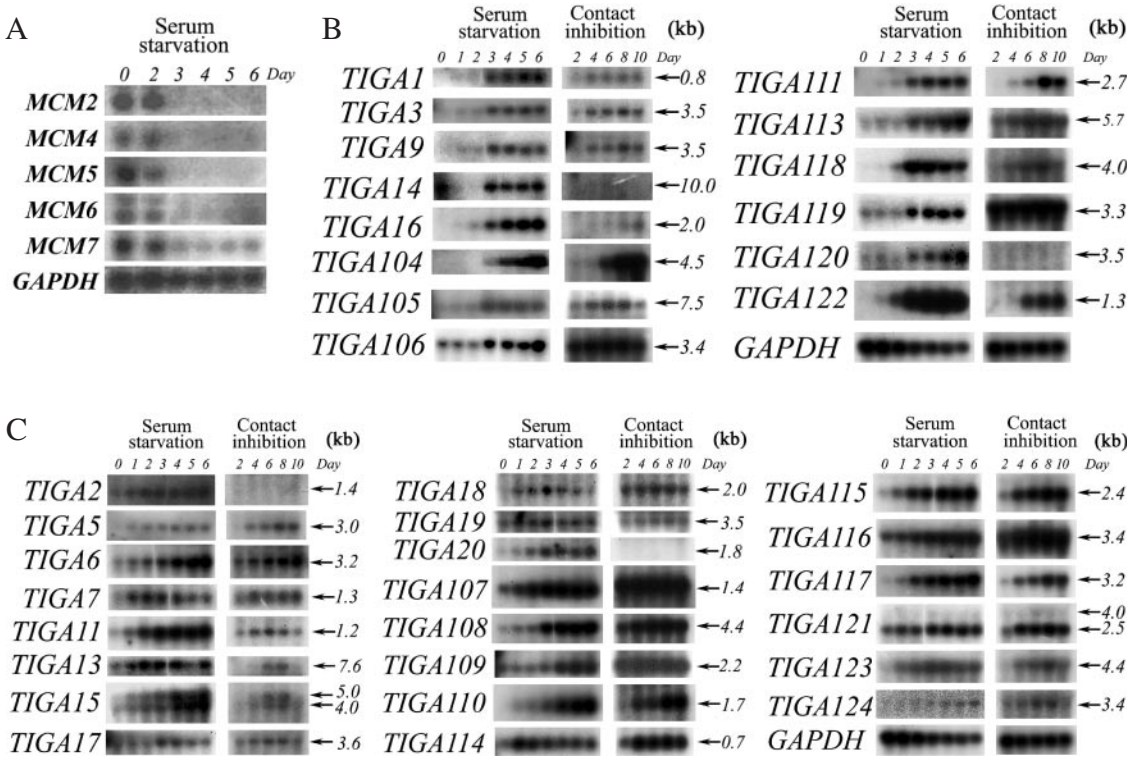

Figure 1. Time-course northern blot analyses of TIG-1 cells. (**A**) Analysis of *MCM* gene expression by TIG-1 cells over 6 days of serum starvation. (B and C) Analysis of the expression of the Group I (**B**) and Group II (**C**) *TIGA* genes (C) by TIG-1 cells over the 6 days of serum starvation (left panels) and the 2–10 days of contact inhibition (right panels). Glyceraldehyde-3-phosphate dehydrogenase (GAPDH) served as a loading control. The size in kilobases (kb) of the mRNA for each *TIGA* gene is shown on the right side of each panel.

Table 1. List of *TIGA* genes

TIGA#	Sequence description
TIGA1	Unknown (This work)
TIGA2	Unknown (RP11-201E8)
TIGA3	Bardet-Biedl syndrome 1 (BBS1)
TIGA4	Unknown
TIGA5	Podocan (IMAGE:4938380)
TIGA6	Transcription factor 21 (TCF21)
TIGA7	Unknown (IMAGE:4184613)
TIGA8	Unknown
TIGA9	Paralemmin
TIGA10	C1 domain-containing phosphatase and tensin-like protein (C1-TEN)
TIGA11	Unknown
TIGA12	Serologically defined breast cancer antigen 84
TIGA13	Mitogen-activated protein kinase kinase kinase kinase 4 (MAP4K4)
TIGA14	Alstrom syndrome 1 (ALMS1)
TIGA15	Pleckstrin homology-like domain, family A (IMAGE:5315177)
TIGA16	DEPP (decidual protein induced by progesterone)
TIGA17	Unknown (IMAGE:3460701)
TIGA18	Kidney predominant protein NCU-G1
TIGA19	TEA domain family member 3
TIGA20	Eukaryotic translation initiation factor 3 (eIF3)
TIGA21	Similar to complement receptor type 2 precursor
TIGA102	Retinoic acid receptor responder3 class II tumor suppressor
TIGA103	Smoothened (SMO)
TIGA104	Alpha-2-macroglobulin
TIGA105	NuMA (nuclear mitotic apparatus protein)
TIGA106	EXT1, putative tumor suppressor gene hormone receptor
TIGA107	OXA1
TIGA108	v-erbA-related ear-3 gene
TIGA109	Similar to human connective tissue growth factor
TIGA110	Bone morphogenetic protein 4 (hBMP-4)
TIGA111	Vitamin D3-upregulated protein 1 (VDUP1)
TIGA112	Gelsolin
TIGA113	TGF-βR8545;α
TIGA114	p8 protein (p8)
TIGA115	Complement compornent 1, r subcomponent (C1R)
TIGA116	Elastin microfibril interface-located protein (EMILIN)
TIGA117	Fibulin1 (FBLN1)
TIGA118	Manganese superoxide dismutase (MnSOD-2)
TIGA119	LIM domain kinase 1(LIMK1)
TIGA120	Similar to C53 CDK5 activator-binding protein (FLJ21805)
TIGA121	Highly similar to nucleobindin precursor (FLJ21805)
TIGA122	Prostaglandin D2 synthase (PTGDS)
TIGA123	Sry-related high mobility group box 4 (SOX4)
TIGA124	LIV-1 protein, estrogen-regulated (LIV-1)

inhibition and serum starvation are known to involve different types of cellular programs (18). For this purpose, we allowed TIG-1 cells to grow to confluency in the presence of 10% FCS. The cells were harvested daily over the following 2–10 days and total RNA was extracted and subjected to northern blots using each *TIGA* cDNA insert as a probe. Based on the time-course variation in the band intensity (mRNA level) of each *TIGA* gene during serum starvation and contact inhibition, we classified the genes into three groups as described below. Notably, the mRNA levels of GAPDH, which were originally going to serve as a loading control, decreased markedly by the 2–3 day transition point in serum starvation. This further demonstrates that after this point, the basic metabolic activity that is supported by glycolysis is downregulated.

The Group I genes (Figure 1B) showed abrupt upregulation of their mRNA levels at 3 days after serum starvation, but no or weak expression at 0–2 days (Figure 1B, left panels). This suggests that these genes play a pivotal role in the induction and/or maintenance of the G0 phase. Many of these upregulations in mRNA levels are probably due to elevated transcription. However, we cannot rule out the possibility that some of these upregulations could also be due to increased mRNA stability, particularly with regard to the genes that showed weak expression at Days 0–2 after serum starvation (e.g. *TIGA105, TIGA106, TIGA113, TIGA119* and *TIGA120*). Given that Day 3 is when the *MCM2-7* mRNAs suddenly disappeared (Figure 1A), these results suggest that cells enter the G0 phase at 3 days after serum starvation; this entry point is likely to involve a distinct mechanism. The other Group I *TIGA* genes showed very low mRNA levels during logarithmic growth (Day 0). *TIGA118* differs from the other Group I genes because while it displayed an abrupt increase in mRNA levels at 2–3 days, its mRNA levels subsequently decreased gradually. This suggests that this gene may participate in the initiation of the G0 phase rather than its maintenance. *TIGA104* [alpha-2-macroglobulin (A2M)] is also remarkable because it shows conspicuous transcriptional induction in both the deep G0-s (Day 6) and the deep G0-c phases (Day 10), although its expression levels are very low until Days 2 or 4 after serum starvation or contact inhibition, respectively. Notably, *TIGA14*, *TIGA16* and *TIGA120* had very low levels of transcriptional induction during contact inhibition, which suggests these genes play specific roles in the G0-s phase. In contrast, *TIGA104*, *TIGA111* and *TIGA122* displayed conspicuous transcriptional induction 6 days after contact inhibition, which suggests that they participate in both G0-s and G0-c.

The Group II genes display a gradual increase in mRNA levels during Days 1–6 of serum starvation (Figure 1C, left panels). Apart from *TIGA110* (bone morphogenic protein 4), these *TIGA* genes were all expressed at low levels at the logarithmic growth phase (Day 0). This suggests that these genes play a role in the vegetative growth phase as well. *TIGA6* (transcription factor 21; TCF21) and *TIGA110* are remarkable because they show conspicuous transcriptional induction in both the deep G0-s (Day 6) and the deep G0-c phases (Day 10). Also notable are *TIGA17* and *TIGA18*, as their mRNA levels peak around Day 3 and then gradually decrease.

The Group III genes displayed greater upregulation of mRNA levels during contact inhibition than during serum starvation (Supplementary Figure S1). These results suggest that the quiescent states caused by serum starvation (G0-s) and contact inhibition (G0-c) differ in a fundamental way. Thus, unlike the Group I genes, the Group II and III genes may participate in growth arrest in general, and thus may be less useful in helping us to understand G0-s.

From these results, we concluded that there are two kinds of G0 phases caused by serum starvation, namely, the shallow G0 (or G0/G1) and the deep G0 phases. We propose an entry point (the G0 gate) that is opened after 3 days of serum starvation but is not necessarily opened by contact inhibition, and that eukaryotic cells are led into the deep G0 phase through this gate.

Some *TIGA* genes are candidate tumor suppressors

Unlike normal somatic cells, cancer cells are destined to repeat the cell cycle indefinitely and cannot be induced to enter the G0 phase by either serum starvation or contact inhibition. Therefore, if some of the *TIGA* genes play pivotal roles in maintaining growth arrest, they are expected to be the tumor suppressor genes. Indeed, we found that the following *TIGA* genes were already reported as candidate tumor suppressor genes.

TIGA6, that encodes a transcription factor 21 (TCF21 = POD1), was reported to be a tumor suppressor gene that is frequently lost in human malignancies (19). POD1 is a basic-helix–loop–helix (bHLH) transcription factor that is highly expressed in the mesenchyme of developing organs and in glomerular visceral epithelial cells (podocytes). Pod1 is essential for the normal development of the testes and ovaries and consequently for sexual differentiation. Pod1 knockout (KO) mice die in the perinatal period with multiple renal defects and Pod1 transcriptionally represses steroidogenic factor 1 (Sf1), which regulates the expression of multiple genes (20). Thus, the expression of Pod1 in the deep G0 phase may either enhance or repress unknown target genes.

TIGA111 encodes vitamin D3-upregulated protein 1 (VDUP1), which is a stress-response gene that is upregulated by vitamin D3 and is considered to be a tumor suppressor gene because it alters p27(kip1) stability by regulating JAB1 (21). Indeed, expression of VDUP1 is frequently lost in tumor tissue and cell lines and its ectopic expression suppresses cellular proliferation along with inducing cell cycle arrest at the G1 phase (22).

TIGA106 encodes exostosin-1 (EXT1) that catalyzes, together with EXT2, the formation of heparan sulfate (HS) chains. Mutations in either *EXT1* or *EXT2* cause hereditary multiple exostosis, which is an autosomal dominant disorder characterized by the formation of a cartilage-capped tumor (23). Thus, the *EXT1* gene is a putative tumor suppressor gene. HS proteoglycans are ubiquitous on the cell surface and in the extracellular matrix, where they regulate signaling molecules such as transforming growth factor-β (TGF-β) by forming HS chains.

TIGA113 encodes the type II receptor of TGF-β. TGF-β has been implicated as both a tumor suppressor and a tumor promoter in many solid epithelial cancers. TGF-β initiates signaling by binding to type I or II receptors and induces G0/G1 arrest through the Smad3-dependent induction of the cyclin-dependent kinase inhibitor p15(Ink4b) (24).

TIGA118 encodes manganese superoxide dismutase-2 (MnSOD-2), a antioxidant enzyme that scavenges superoxide anions and is an important modulator of nitric oxide bioavailability. Moreover, treatment of antioxidant induces the G1 cell cycle arrest (25). SOD-2 has been postulated to be a tumor suppressor and its identification as a *TIGA* gene is consistent with previous observations showing that overexpressing MnSOD activity inhibits the growth of cultured human prostate carcinoma cells (26), and that SOD-2 is one of the downstream mediators of the senescence-associated tumor-suppressing effect of mac25/IGFBP-rP1 (27).

TIGA1 encodes a small protein with a single transmembrane domain

To understand the physiological significance of the *TIGA* genes we identified, we selected *TIGA1* for further analysis. This gene was selected because it maps to the 5q21–q22 region where the adenomatosis polyposis coli (APC) gene is localized. The deletion of the 5q21-q22 region is believed to cause familial adenomatous polyposis (28). Since loss of heterozygosity (LOH) in the 5q21–q22 region has also been frequently observed in small-cell lung carcinoma (SCLC) as well as non small-cell lung carcinoma (NSCLC), it has been predicted that this region also contains unknown tumor suppressor genes other than APC; *TIGA1* is identical to one of the candidates, LI33 (29).

TIGA1 belongs to the Group I *TIGA* genes and shows no expression at the mitotic growth phase (Day 0 of Figure 1B), very low expression on Days 1–2 of serum starvation, and then abrupt transcriptional induction on Day 3 (Figure 1B). In contact inhibition, while *TIGA1* did display weak transcriptional induction at Day 3, its expression levels remained constant thereafter. Thus, *TIGA1* seems to function specifically in response to serum starvation. It is notable that the *TIGA1* cDNA sequences registered in the databank contain a large number of mutations in not only the non-coding region but also the ORF (Supplementary Figure S2). Moreover, some of the mutations caused amino acid changes or generated stop codons that could have deleterious effects on Tiga1 function. On the basis of this, we surmised that *TIGA1* mutations may be involved in lung carcinogenesis. Our reasoning will be discussed later.

TIGA1 encodes a small protein (Tiga1; 120 amino acids) that has a transmembrane domain without a signal peptide motif (Figure 2A). Northern blot analysis indicated that the *TIGA1* gene generates two transcripts. The 0.8 kb transcript that can produce Tiga1 protein is ubiquitously detected in all human tissues examined (Figure 2B), which is logical because all of these tissues contain many cells in the quiescent state (G0 phase) and *TIGA1* mRNA is abundant in this state (Figure 1B). It remains unknown why the 2.9 kb transcript is observed faintly in many tissues and strongly in the brain, pancreas, spinal cord and kidney (Figure 2B). We also examined the expression of the *TIGA1* gene in lung cancer cell lines and found that the *TIGA1* mRNA levels were almost undetectable in EBC-1, Lu-134-A and Lu-140 and very low in Lu-65, Lu-130 and Lu-135 (Figure 2C). Unlike all the other lines, Lu-139 displayed high levels of *TIGA1* expression primarily because this cell line alone did not display LOH around the *TIGA1* gene as will be shown later (Figure 7C) and thus has an extra allele.

Western blot analysis of Tiga1 expression

To analyze Tiga1 protein expression, we raised a polyclonal anti-Tiga1 rabbit antibody by using affinity-purified GST-Tiga1 protein as the antigen. To determine whether the antibody specifically recognizes Tiga1 protein, we generated *Escherichiacoli* cells transfected with a GST-Tiga1-expressing plasmid. These cells were incubated at either 20 or 37°C with isopropyl β-D-thiogalactoside (IPTG), which induces GST-Tiga1 protein expression. Cells that were not

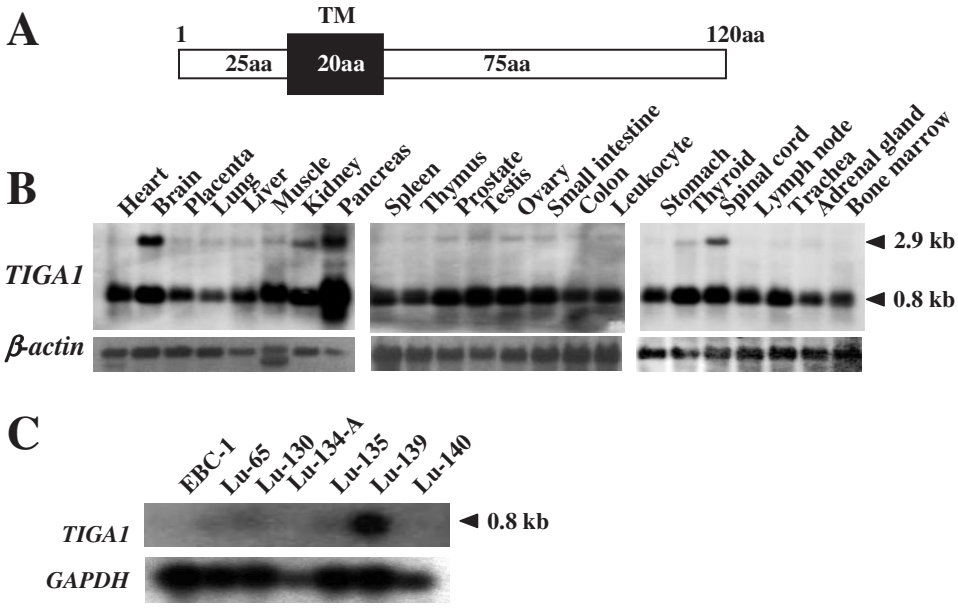

Figure 2. Structure and expression of *TIGA1* in human tissues and human cancer cells. (**A**) Schematic representation of the Tiga1 protein (120 amino acids) that shows its transmembrane (TM) region. (**B**) Analysis of *TIGA1* expression in human multiple tissue Northern blots (Clontech). β-actin cDNA served as a loading control. (**C**) Northern blot analysis of *TIGA1* expression in human lung cancer cells. GAPDH served as a loading control. The northern blots were probed with ^{32}P-labeled *TIGA1* cDNA.

incubated with IPTG served as a control. Parallel Western blot analyses using either an anti-GST antibody or the affinity-purified anti-Tiga1 antibody revealed both antibodies recognized bands that had the expected size of the GST-Tiga1 protein (the 27 kDa GST tag plus 13kDa = 40 kDa). Thus, the anti-Tiga1 antibody specifically recognizes Tiga1 protein (Figure 3A). Since incubation of *E.coli* at 37°C appeared to generate degraded products, we incubated the cells at 20°C for large scale preparation of GST-Tiga1 protein.

We used the anti-Tiga1 antibody to analyze the cell extracts of TIG-1 cells that had entered G0 phase due to serum starvation. Western blot analysis of these extracts revealed that the antibody recognized a band at 26 kDa (Figure 3B), which is larger than the expected size of Tiga1 (13 kDa). However, since the band intensity increased during serum starvation, this band appears to be the band for Tiga1. To confirm this, we performed another Western blot analysis using a different set of size markers and again detected a single band at 26 kDa (Figure 3C). It is likely that this band contains Tiga1 protein that has been modified in some way. Thus, it appears that *TIGA1* is also regulated at the posttranscriptional level, as both its protein levels are upregulated and its protein structure is modified.

Ectopic *TIGA1* expression inhibits the colony-forming ability of tumor cells

To determine if the transcriptional induction of *TIGA1* after serum deprivation causes the cellular growth arrest, we evaluated the effect of ectopic expression of *TIGA1* on the proliferation of tumor cells, as these cells are unable to enter the G0 phase. To do so, we performed colony formation assays. Thus, we transiently transfected the lung cancer cell line EBC-1, which does not express any *TIGA1* transcripts (Figure 2C), with an *hemagglutin (HA)-TIGA1*-expressing vector (pcDNA3-HA-TIGA1) that harbors a neomycin resistance gene. The transfected cells were cultured for 2 weeks in medium containing G418 to select the cells, and number of survival colonies were counted. As a positive control, EBC-1 cells were transfected with a plasmid harboring p53 cDNA, which induces growth arrest. As a negative control, the cells were transfected with plasmid alone. As shown in Figure 3, the EBC-1 cells that constitutively express Tiga1 show a significant reduction in both colony number and size, as compared to cells transfected with vector alone (Figure 4A). Moreover, *TIGA1* expression reduced the colony-forming efficiency by 70% compared to cells transfected with the vector alone (Figure 4B). This level of reduction was slightly weaker than that induced by transfection with wild-type p53. These results indicate that ectopic expression of *TIGA1* inhibits cell proliferation, which suggests that *TIGA1* may trigger the growth arrest process.

Ectopic *TIGA1* expression inhibits tumor growth in soft agar

To know the role of *TIGA1* as a tumor suppressor, we examined whether ectopic expression of *TIGA1* could suppress the anchorage-independent growth. To introduce the *TIGA1* gene into human cancer cell lines, we made an amphotropic retrovirus carrying with *TIGA1* gene. *TIGA1* retrovirus and control retrovirus were introduced into the bladder carcinoma cell line T24 and the osteosarcoma cell line SaOS-2. As shown in Figure 5A, *TIGA1* infected cells inhibited the growth of these cells in soft agar.

We also examined the effect of *TIGA1* overexpression in the expression-inducible EcR-293 cell line that constitutively expresses the recombinant ecdysone receptor (30). Thus,

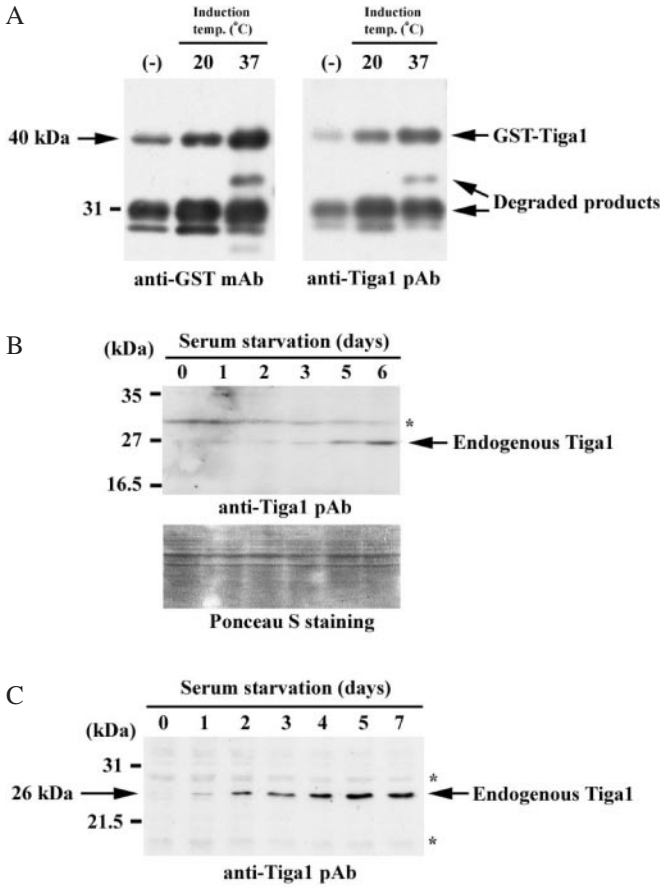

Figure 3. Western blot analysis using an anti-Tiga1 antibody. (**A**) Anti-Tiga1 antibody specifically recognizes Tiga1 protein when *Escherichiacoli* cells that can express GST-Tiga1 protein were incubated in the absence (−) or presence of isopropyl β-D-thiogalactoside (IPTG) at 20 or 37°C to induce expression of GST-Tiga1 protein. (**B**) Western blot analysis using this anti-Tiga1 antibody yielded a band for endogenous Tiga1 protein at 26 kDa. An asterisk denotes the putative nonspecific band. Ponceau S staining of the polyacrylamide gel is presented as a loading control. (**C**) Western blot analysis with a new set of size markers. The reproducibility of the migration of the band for Tiga1 at 26 kDa was confirmed. Asterisks denote the putative nonspecific band.

TIGA1 cDNA was inserted in the pIND vector and transfected into EcR-293 cells and selected for 2 weeks in G418 and zeocin containing medium. Drug resistant cells were pooled and expression of Tiga1 protein was induced by ecdysone successfully as shown in Figure 5B. The ectopically expressed Tiga1 protein migrated at the rate expected for a 120 amino acid protein, which suggests that Tiga1 is not post-translationally modified in rapidly growing EcR-293 cells. Using these cells, we examined the effect of overexpression of *TIGA1* on cell proliferation and anchorage-independent growth. In the soft agar assay, ecdysone-induced *TIGA1* expression significantly inhibited the growth of the EcR-293 cells (Figure 5A). The introduction of vector alone had no apparent effect. Figure 5C shows a typical image exemplifying the Tiga1-mediated inhibition of EcR-293 cell growth in soft agar. We also showed that HA-Tiga1 expression induced by ecdysone inhibited the growth of pIND-HA-Tiga1-transfected EcR-293 cells that were cultured in normal growth medium in the presence of ecdysone (Supplementary Figure S3). Thus, ectopic overexpression of *TIGA1* inhibits both the anchorage-dependent and independent growth of tumor cells.

Subcellular localization of Tiga1

We next investigated the subcellular localization of Tiga1 by constructing a GFP-Tiga1 fusion protein-expressing plasmid and transfecting COS-7 cells with it. The growth of the COS-7 cells looked normal for a few days after transfection but the growth rate then decreased gradually and eventually stopped altogether (data not shown). When we observed the subcellular localization of GFP-Tiga1 2 days after transfection, we found that it had a granule-like cytoplasmic distribution (Figure 6A, upper panel). This suggests that Tiga1 is localized in the microsome of the cytoplasm but not in the cellular membrane. This distribution was distinct from the diffuse distribution of EGFP throughout the cytoplasm in GFP-expressing recombinant cells (Figure 6A, lower panel). The localization of GFP-Tiga1 in the mitochondria was confirmed by staining GFP-Tiga1-expressing HeLa cells with the mitochondrial staining marker MitoTracker. As expected, when GFP-Tiga1 was exogenously expressed in HeLa cells, it co-localized with MitoTracker (Figure 6B).

We next performed a protease protection assay to determine the direction Tiga1 is inserted in the mitochondrial membrane. HeLa cells were transfected with a plasmid

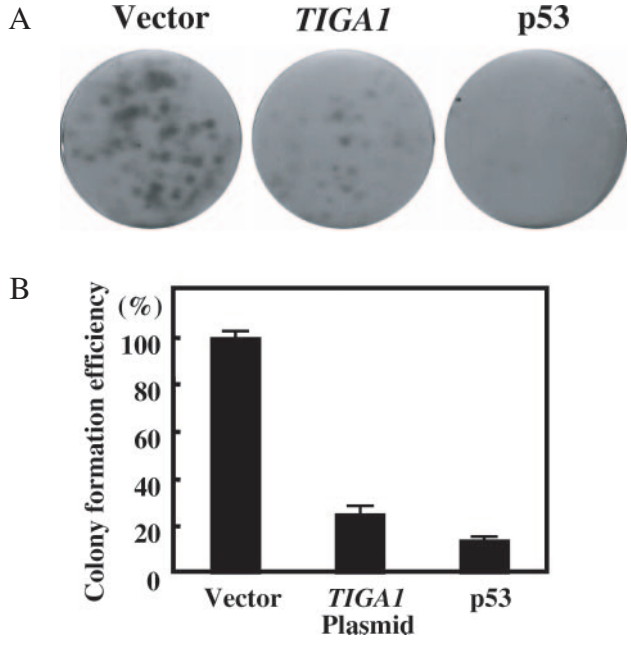

Figure 4. Ectopic expression of *TIGA1*, like *p53*, inhibits the colony-forming ability of EBC-1 cells. (**A**) Equal amounts (2 μg) of plasmid encoding a neomycin resistance gene alone (pcDNA3-HA, vector) or the same vector containing *TIGA1* (pcDNA3-HA-TIGA1) or *p53* (pcDNA3-Flag-p53) cDNAs, were transfecte into EBC-1 cells. After growth for 2 weeks in medium containing G418, the plates were fixed and stained with crystal violet to identify the surviving colonies. (**B**) The reproducibility of the result was confirmed by repeating the experiment three times. Bar graphs that summarize the results from three independent experiments (each in triplicate). Error bars indicate the SDs of the mean.

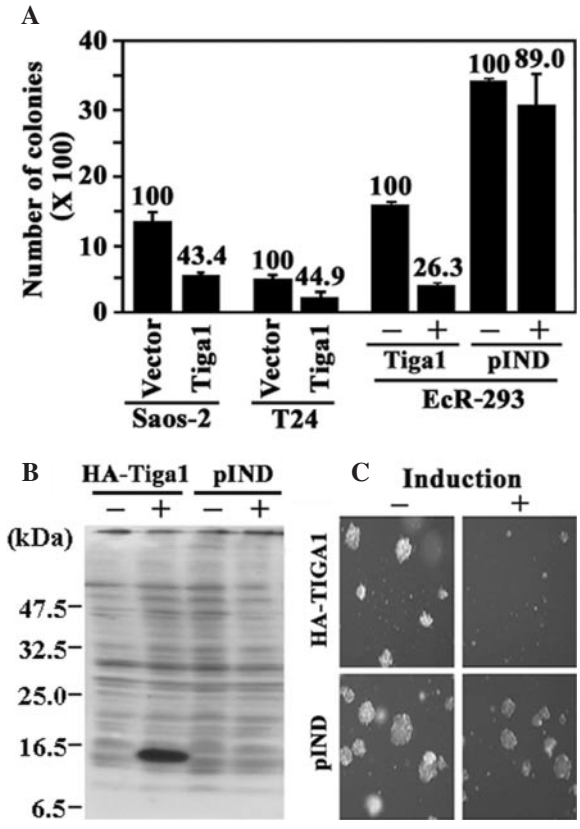

Figure 5. Ectopic Tiga1 expression suppresses the anchorage-independent growth of Saos-2, T24 and EcR-293 cells. (**A**) Saos-2 and T24 cells were infected by the pCXbsr vector virus (Vector) or the recombinant virus containing HA-tagged Tiga1 (Tiga1). Ecdysone-inducible 293 (EcR-293) cells were stably transfected with the pIND vector alone (pIND) or pIND-HA-Tiga1 (Tiga1) and treated with (+) or without (−) 1 μM muristerone A, a synthetic analogue of ecdysone. All cells were inoculated into soft agar, and the growing colonies were scored after incubation for 10 days. The number above each bar in the graph indicates relative colony formation efficiency. The reproducibility of the result was confirmed by repeating the experiment three times. Error bars indicate the SDs of the mean. (**B**) The colonies generated by the EcR-293 cells bearing the pIND vector or pIND-HA-Tiga1 as shown in (A) were photographed. (**C**) Induction of HA-tagged Tiga1 expression in EcR-293 cells by muristerone A. The cell lysates from the EcR-293 cells shown in (A) and (B) were resolved by SDS–PAGE, followed by western blotting with anti-HA antibody.

expressing Tiga1 that was tagged at its N-terminus with 6Myc (6Myc-Tiga1). The cells were digested with various amounts of trypsin in the presence or absence of Triton X-100 for 15 min, boiled in sample buffer and the lysates were subjected to Western blot analysis with the anti-Myc antibody. The presence of Triton X-100 itself had no effect on the size of the 6Myc-Tiga1 protein (Figure 6C, lanes 1 and 5) but 0.5 and 1 μg trypsin digestion completed digested 6Myc-Tiga1. However, while 0.25 μg trypsin failed to destroy 6Myc-Tiga1 in the absence of 1% Triton X-100 (Figure 6C, lanes 2–4), the presence of Triton X-100 facilitated the trypsin-mediated destruction of 6Myc-Tiga1 (Figure 6C, lanes 2–6). This result suggests that the N-terminus of Tiga1 is localized in the mitochondria while its C-terminus is in the cytoplasm.

Both the N- and C-terminal portions of Tiga1 are responsible for its mitochondrial localization and cellular toxicity

To examine which region of Tiga1 is required for its mitochondrial localization, we fused GFP to various Tiga1 deletion constructs (Figure 7A) and expressed them in HeLa cells. We found that most of the intact (full-size) Tiga1 fused with GFP (denoted as Tiga1-full in Figure 6B) colocalized with cytochrome *c*, which is also in the mitochondria as revealed by MitoTracker (Figure 7B). While some of the GFP-Tiga1-a and GFP-Tiga1-b proteins also colocalized with cytochrome *c*, they did so much less frequently than GFP-Tiga1-full. Almost no colocalization was observed for the GFP-Tiga1-c protein. These results indicate that while both of the N-terminal and C-terminal regions around the transmembrane domain are required for the mitochondrial localization of Tiga1, the former plays a more important role.

During these experiments, we noted that few of the cells expressing GFP-Tiga1 were viable, unlike the cells that expressed the GFP vector alone. Western blot analysis also showed that expression of GFP-Tiga1 was very low compared to GFP alone (Figure 7C). This suggests that GFP-Tiga1 is toxic to cultured cancer cells. To eliminate the possibility that the low expression of GFP-Tiga1 was due to low transcription-translation efficiency, we compared the frequencies of the GFP-expressing cells and the live cells that carry each deletion mutant form of Tiga1. When vector alone was expressed, >60% of the cells showed the GFP signal (Figure 7D). In contrast, a very low frequency of

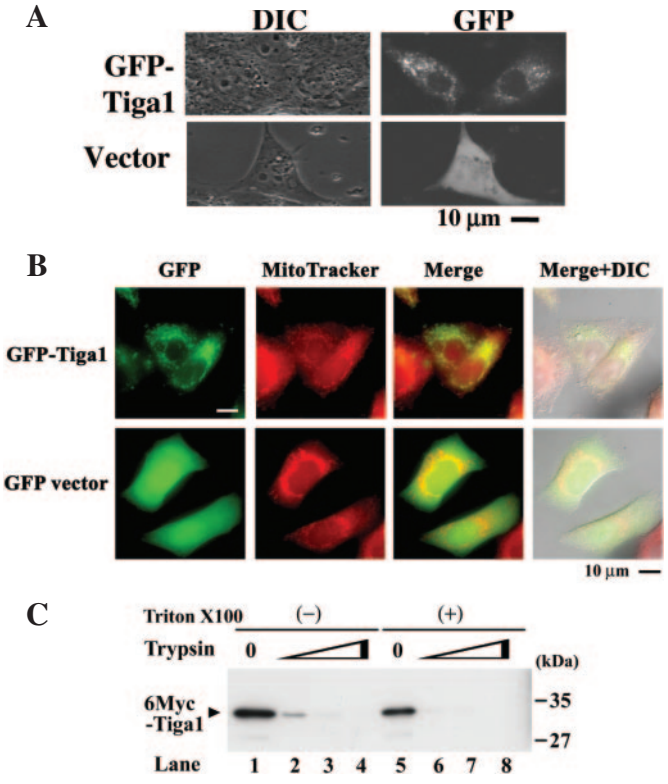

Figure 6. Subcellular localization of GFP-tagged Tiga1. (**A**) Microscopic images of the fluorescence emitted by the GFP proteins (right). COS-7 cells were transfected with plasmid DNAs expressing GFP-tagged Tiga1 or GFP alone and examined under a microscope after 48 h of incubation. The differential interference contrast (DIC) images are shown on the left. (**B**) Microscopic images of the fluorescence emitted by GFP or MitoTracker in HeLa cells transfected with a plasmid expressing GFP-tagged Tiga1. The cells were treated with MitoTracker before chemical fixing. Merged images are also shown. The GFP and MitoTracker signals are green and red, respectively, and the merged signals are yellow. (**C**) Protease protection assay to determine the orientation of Tiga1 in the mitochondrial membrane. HeLa cells expressing 6Myc-Tiga1 were digested with various amounts of trypsin (lanes 1 and 5, 0 μg/ml; lanes 2 and 6, 0.25 μg/ml; lanes 3 and 7, 0.5 μg/ml; lanes 4 and 8, 1 μg/ml) in the absence (lanes 1–4) or presence (lanes 5–8) of 1% Triton X-100, followed by boiling and Western blot analysis with an anti-Myc antibody (PL14).

cells displayed the GFP signal when they expressed GFP-Tiga1-full or GFP-Tiga1-c. In contrast, cells expressing GFP-Tiga1-a or GFP-Tiga1-b showed less severe toxicity. This is independent of their co-localizations with cytochrome *c*, as described above (Figure 7A). Thus, the entire C-terminus region is responsible for the cellular toxicity of Tiga1.

Analysis of the microsatellite marker *ENDL-1* reveals LOH of the *TIGA1* allele in cancer cells

It has been reported that LOH at 5q21–22, which contains the *TIGA1* allele, is frequently observed in the cell lines and tissues of lung cancer patients (28). To investigate whether LOH is also detected at a locus proximal to *TIGA1* gene, we designed a new microsatellite marker, namely, *ENDL-1*, which consists of $(TA)_{23}$ and $(CA)_{11}$ repeats and is located ~75 kb from the 5′ end of the *TIGA1* gene (Figure 8A and B). We subjected small-cell lung cancer (SCLC), non SCLC (NSCLC) and various other cell lines to LOH analysis with *ENDL-1*. Normal TIG-1 cells exhibited two bands that correspond to the two alleles from the mother and father. In contrast, a single band was detected for most of the SCLC and NSCLC lung cancer cell lines we tested, namely, Lu-24, Lu-130, Lu-134, Lu-135, Lu-140 and H69 of the SCLC lines and EBC-1, Lu-65, PC-3, PC-7 and PC-10 of the NSCLC lines. Only one SCLC (Lu-139) and one NSCLC (A549) line had both alleles. Moreover, we also found LOH in other cancer cell lines, namely, MCF-7, Jurkat and HL60 (Figure 8C). That both leukemia cell lines (Jurkat and HL60) showed LOH is consistent with a study that found a high degree of LOH in this region in patients with acute myeloid leukemias and acute lymphoblastic leukemias (31). Thus, we conclude that the region of the genome that is in the vicinity of the *TIGA1* gene is frequently deleted in many cancer cell lines and that *ENDL-1* can serve as an informative microsatellite marker for this LOH.

DISCUSSION

Serum starvation and contact inhibition induce distinct G0 phases

In the present study, we isolated 44 *TIGA* genes from human primary culture fibroblast (TIG-1) cells whose mRNA levels are upregulated by serum starvation and/or contact inhibition. Our isolation of *TIGA* genes here has clarified two issues. First, while some *TIGA* genes are upregulated by both serum starvation and contact inhibition, other *TIGA* genes respond to one or the other stimulation but not both (Figure 1 and Supplementary Figure 1S). For example, *TIGA2*, *TIGA14*, *TIGA20* and *TIGA120* may be involved in G0-s alone because contact inhibition had little to no effect on the expression of these genes. In contrast, the Group III *TIGA* genes may be predominantly involved in G0-c alone because they exhibited very low responses after serum starvation (Supplementary Figure 1S). Meanwhile, *TIGA6*, *TIGA104*, *TIGA110*, *TIGA111*, *TIGA117* and *TIGA122* may be involved in both G0-s and G0-c phases since both serum starvation and contact inhibition induced their strong responses. Thus, while G0-s and G0-c are partly regulated by the same genes, distinct mechanisms that are mediated by specific genes are also involved. Second, we identified a point of entry into the deep G0 phase at Day 3 of serum starvation. This point is referred to here as the 'G0 gate'. Fourteen *TIGA* genes (Group I) are abruptly upregulated at the G0 gate and their mRNA levels remained almost constant afterwards (Figure 1B and C). Notably, the expression of the six *MCM2-7* genes that are induced at the initiation of S phase of the mitotic cell cycle (16) is abruptly downregulated after Day 3 of serum starvation (Figure 1A). This further supports the existence of a 'G0 gate' at which point the expression of growth-promoting genes cease.

The definition of the G0 gate as the expression of the 14 *TIGA* genes after 3 days of serum starvation helps us to better understand the previously ambiguously defined G0 phase. Earlier studies have shown that G0 can be induced by short serum starvation, namely, a few hours or less (2,32). In these papers, the evidence for G0 arrest was that the cells needed time (6–8 h) to return to the cell cycle. This feature

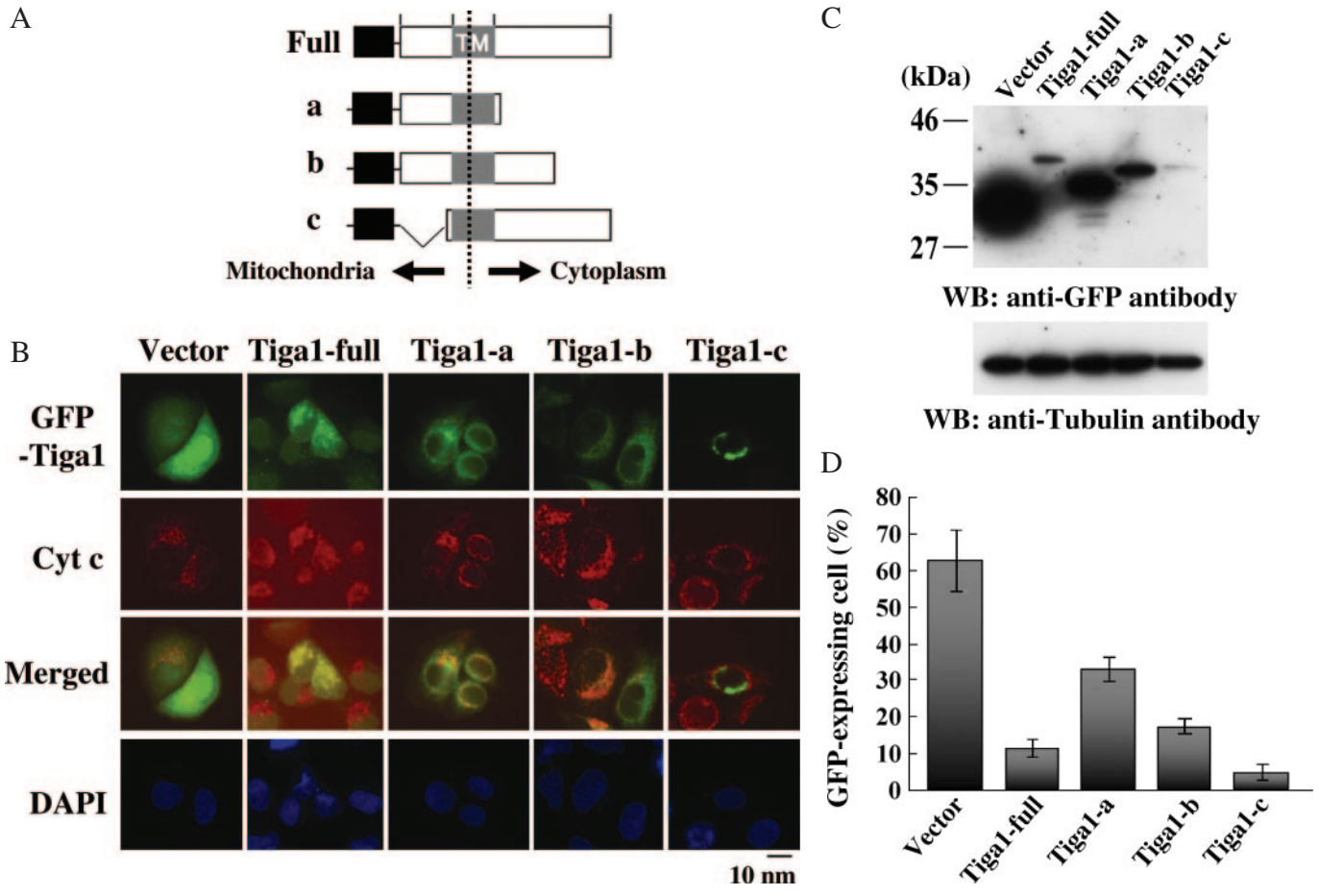

Figure 7. Both its N- and C-terminal regions are required for the mitochondrial localization of Tiga1. (**A**) Schematic presentation of GFP-fused Tiga1 deletion constructs. The N-terminal portion of Tiga1 is within the mitochondria while its C-terminal portion is in the cytoplasm. (**B**) Microscopic images of HeLa cells that express the various GFP-Tiga1 deletion constructs or GFP vector alone. GFP-Tiga1 proteins were visualized by staining with anti-GFP antibody (green) while cytochrome *c* was detected by anti-cytochrome *c* antibody (Promega) and Alexa 594-conjugated anti-mouse IgG antibody (red). The nuclei were stained with DAPI (blue). (**C**) Western blot analysis of the total cell extracts obtained from HeLa cells transfected with the GFP-fused Tiga1 deletion constructs. The GFP-Tiga1 fusion proteins were detected by anti-GFP antibody (clone J1). Tubulin served as a loading control. (**D**) Percentages of cytochrome *c*-expressing cells versus GFP-expressing cells for each plasmid construct.

also characterizes the G0 arrest that is induced after 3 days of serum starvation. On the basis of these observations, we postulate that the G0 phase that induced after a few hours of serum starvation should be called 'shallow G0' (or G0/G1 phase) while the G0 phase generated by 3 days of serum starvation should be called 'deep G0'. Since the G0 gate only opens after 3 days of serum starvation, it separates the shallow G0 phase from the deep G0 phase. Further studies will be needed to determine how the shallow and deep G0 phases differ. With regard to the role Tiga1 protein plays in shallow and deep G0, we know that its levels are dramatically increased in deep G0 (Figures 1B and 3). As described below, it is likely to act in the mitochondria to control the fuel consumption of the cells, thereby maintaining the low metabolism of the cells in shallow G0 and more importantly in deep G0.

Recent genome-wide analysis has revealed a large number of genes that are either upregulated or downregulated upon serum starvation or contact inhibition (33). To our surprise, none of the *TIGA* genes were not detected by this analysis except for *TIGA20* (eIF3) (which, unlike our observations, is listed as a G0-downregulated gene). Moreover, this study did not find that *MCM5* is downregulated upon serum starvation, although it was listed it as a gene that is upregulated by contact inhibition. It is not known whether these discrepancies are due to differences in the experimental systems used. Since these authors did not confirm their DNA chip data by Northern blot analysis or quantitative RT–PCR, it is difficult to compare their results with ours.

Some *TIGA* genes regulate cell growth

By examining the structure of the *TIGA* gene products, we noticed that some of them are involved in regulation of cell growth. For example, *TIGA20* (=eIF3; eukaryotic translation initiation factor 3) is known to stimulate the recruitment of the eIF2-GTP-Met-tRNAiMet ternary complex to the 40S ribosome along with other initiation factors, including eIF1, eIF5 and eIF1A (34). Consequently, it may enhance the translation of the mRNAs that are left intact in G0-s phase cells. Its expression is probably important in G0-s because some mRNAs are present in G0 cells at markedly reduced

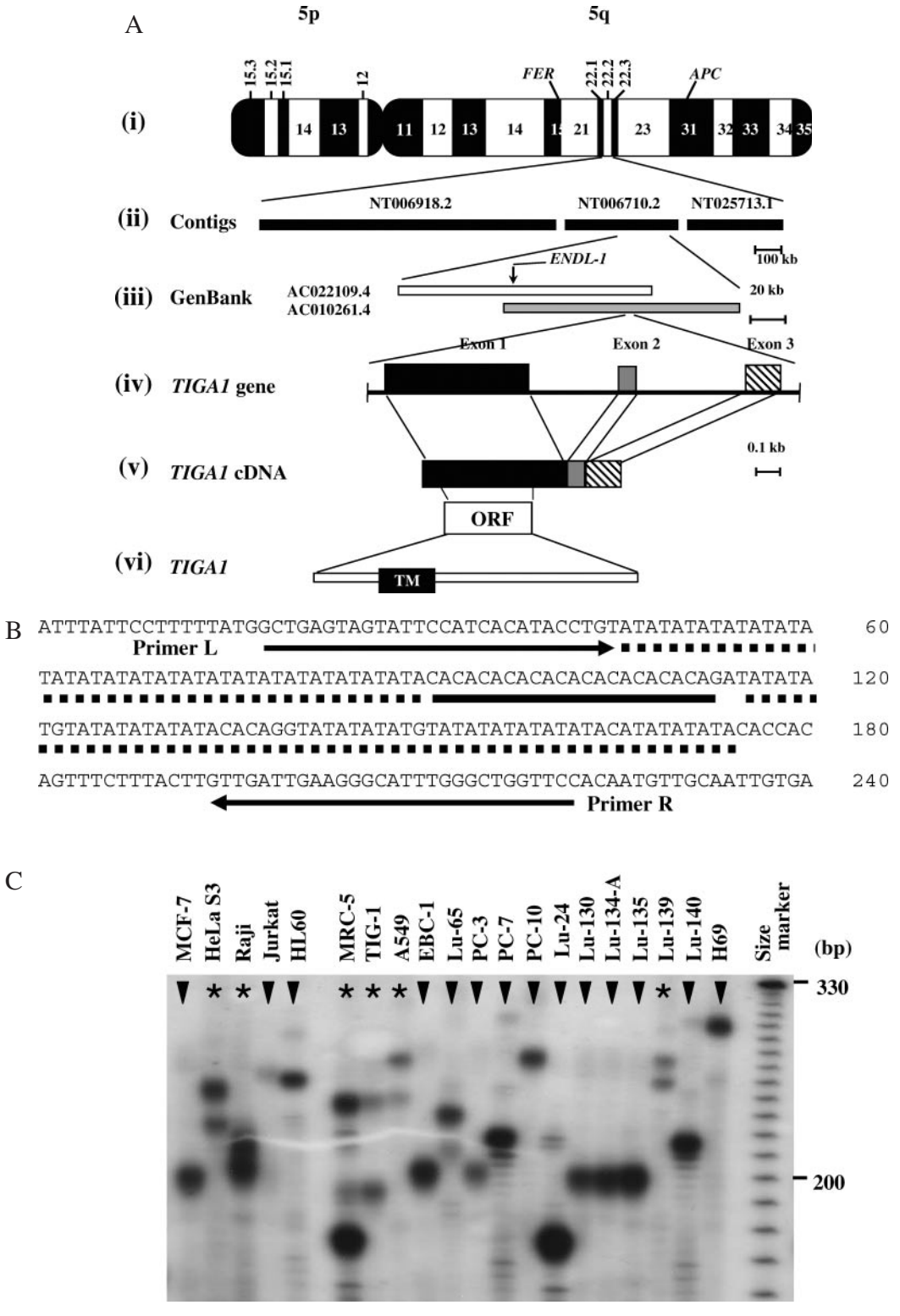

Figure 8. The *TIGA1* gene locus in cancer cells exhibits LOH. (**A**) Schematic depiction of the chromosomal localization of the *TIGA1* gene. (i) The banding pattern of human chromosome 5 that illustrates the localization of *TIGA1* in 5q22.2. (ii) Map of chromosome 5 and the corresponding contigs in 5q22.2. The locations of the *FER* tyrosine kinase gene and the *APC* gene, which are frequently deleted in cancer cells (28), are indicated. (iii) Two DNA fragments from GenBank cover part of the contig NT006710.2. A vertical arrow indicates the locus of the microsatellite marker *ENDL-1*. (iv–vi) Schematic representation of the *TIGA1* gene, *TIGA1* cDNA and Tiga1 protein. *TIGA1* is composed of three exons and encodes an ORF of 120 amino acids (aa). (**B**) DNA sequences around the microsatellite marker *ENDL-1* that were used for the PCR amplifications. The PCR primer sequences are shown by horizontal arrows. Dotted and bolded underlines denote the $(AT)_{22}$ and $(CA)_{11}$ repeats, respectively. (**C**) Analysis of LOH at *ENDL-1* in normal (TIG-1) or cancer cells. Cells showing the presence of two alleles are denoted by asterisks at the top of each lane, while cells showing only one allele (i.e. LOH) are indicated by vertical arrowheads. The electrophoretic patterns of the radiolabeled probes in 6% polyacrylamide gel are shown.

quantities, and the enhanced activation of their translation is needed to keep the cells alive in G0-s. Notably, eIF3 is not elevated in G0-c phase cells, which confirms the possibility that the G0-s and G0-c phases are regulated differently.

TIGA16 (=DEPP; decidual protein induced by progesterone) encodes one of the progesterone or androgen-inducible genes that can enhance the levels of phosphorylated Erk, which in turn activates the Elk-1 transcription factor (35). Thus, DEPP may act as a G0 signal that regulates the silencing of many target genes. *TIGA9* encodes paralemmin, a novel lipid-anchored protein that is highly expressed in neuronal plasma membranes. It has been implicated as a potent modulator of cellular cAMP signaling within the brain by specifically interacting with the third intracellular loop of the D3 dopamine receptor (36).

TIGA104 encodes A2M, which is an abundant plasma/extracellular space protein that also regulates proteinase and growth factor activities. *A2M* gene transcription is induced by IL-6 through the action of STAT3 (37). Since its expression is dramatically induced in both the deep G0-s and G0-c phases, A2M may serve to fill the extracellular space to maintain the G0 phase or to inhibit the activity of unknown growth-promoting protease(s).

TIGA105 encodes the nuclear mitotic apparatus protein, which cross-links microtubule ends at spindle poles and is a substrate for covalent modification by tankyrase-1, a PARP [poly(ADP-ribose) polymerase] that is required for the assembly of bipolar spindles in mitosis (38). *TIGA120* encodes a protein that is similar to C53 (Cdk5 activator-binding protein). C53 serves as an important regulatory component of the G(2)/M DNA damage checkpoint that is generated in response to genotoxic stress (39). Since C53 overexpression promotes Cdk1 activity and the nuclear accumulation of cyclin B1, the induction of *TIGA120* in only the G0-s phase suggest that it may play a role in modulating Cdk/Cyclin function to maintain the quiescent state.

TIGA122 encodes the lipocalin-type prostaglandin D2 synthase (PTGDS), which is a key enzyme in the arachidonic acid metabolism pathway, whose enzyme-derived metabolites inhibit cell proliferation (40). It appears that this enzyme is required for G0 cells to remain in the quiescent state because its expression is not only increased when the cells entered the deeper G0-s phase, it is also abruptly induced after 6–10 days of contact inhibition. This observation is interesting because an anti-inflammatory drug NS-398 that inhibits prostaglandin synthesis reduced cell proliferation in ovarian carcinoma cells by inducing G0/G1 cell cycle arrest (41). Our result suggests that the bona fide target of NS-398 may be PTGDS rather than COX-2.

Mutations of some *TIGA* genes cause hereditary disease

We also noticed that some *TIGA* genes are the responsible genes for human hereditary diseases, which indicates that their functions are important for proper maintenance of the body. For example, *TIGA3* (=*BBS1*) is one of the six genes whose dysfunction causes the genetically heterogeneous disorder Bardet-Biedl syndrome (BBS), which is characterized primarily by retinal dystrophy, obesity, polydactyly, cognitive impairment and gonadal and renal dysgenesis (42). BBS1 (593 aa) is ubiquitously expressed in human tissues, probably because most of the cells in the body are in G0 phase. BBS patients and BBS1-defective Tubby mice have defects in ciliated neuron function and obesity, suggesting a metabolic signaling axis from ciliated neurons to fat storage tissues. Studies on the BBS1 homolog in *Caenorhabditis elegans* revealed its coordinate regulation with a 3-ketoacyl-coA thiolase that acts in fat storage tissue (43).

TIGA14 encodes ALMS1, a protein whose dysfunction causes the autosomal recessive disease Alstrom syndrome, which is characterized by cone-rod retinal dystrophy, cardiomyopathy and type 2 diabetes mellitus (44,45). The *ALMS1* gene encodes a large protein of 4169 amino acids containing a large tandem-repeat domain comprised of 34 imperfect repetitions of 47 amino acids. Six different mutations in *ALMS1* were detected in seven families with Alstrom syndrome, which confirms that *ALMS1* is the gene that underlies this syndrome (44,45). While *ALSM1* is ubiquitously expressed in human tissues as detected by RT–PCR (44), it is highly expressed in the heart, placenta, skeletal muscle, pancreas and testis, as determined by Northern blot analysis (45).

TIGA119 encodes LIMK1, which commonly suffers deletion in Williams syndrome (WS). WS is characterized by dysmorphic features, mental retardation or learning difficulties, elastin arteriopathy, and striking neurocognitive and social-behavioral abnormalities (46). LIMK1 plays an important role in cell motility by phosphorylating and inactivating the actin depolymerization factor cofilin, and regulates actin cytoskeletal changes (47). It is also involved in microtubule destabilization (48).

Putative function of the Tiga1 protein and evolution of the *TIGA1* gene

To determine whether the ectopic expression of the *TIGA* genes would inhibit the perpetual growth of cancer cells, we selected *TIGA1,* one of the uncharacterized genes, for further functional analysis. We found that the ectopic expression of *TIGA1* inhibited not only tumor cell growth in medium (Figure 4 and Supplementary Figure S3) but also anchorage-independent tumor cell growth in soft agar (Figure 5). We also found that Tiga1, which is a small protein with a single transmembrane domain, is localized in the mitochondria (Figures 6 and 7). Moreover, ectopic expression of *TIGA1* was toxic to cultured cancer cells. This may be due to the aberrant cytochrome *c* release and mitochondrial membrane permeability that is induced by ectopic Tiga-1 expression. As discussed below, the homology of Tiga1 to cyanate permease and the ABC transporter of bacteria supports the notion that Tiga1 is a regulator of ion transport in the mitochondrial transmembrane. This is also suggested by the fact that the growth inhibition and G0/G1 arrest induced by the histone deacetylase inhibitor MS-275 is caused by the loss of mitochondrial transmembrane potential (49). Furthermore, by using the *ENDL-1* microsatellite marker, we could detect LOH around the *TIGA1* gene region in many cancer cells, including SCLCs and NSCLCs (Figure 8). Thus, *ENDL-1* may be an useful marker to detect deletions in chromosome 5q21–22.

Curiously, *TIGA1* is found only in primates and no homologous genes were found in any other vertebrates. However, homologous proteins were found in yeast and bacteria

Unnamed protein product of lipolytic yeast [*Yarrowia lipolytica*] XP_503129 (1079 aa)

```
Tiga1    4 PAPPSRSRTVGPSTCRKALWDGSLSF---LPFGASLLWFLLWVLWDGAWLWPRGLSRRGAGRGNAATLSLVSR 73
           P  P  S   G    ++ L D + ++   LPF   L++ L     D AWLWP   +RR AGR  A+ L L+ +
Sbjct 242 PENPDESIAEGRKLAKEYLGDTTKAYKQQLPFADGLVYALGNCHIDTAWLWPFAETRRKAGRSWASQLELIDK 314
```

Hypothetical protein Paer03003214 [*Pseudomonas aeruginosa* UCBPP-PA14] ZP_00139114 (138 aa)

```
Tiga1    4  PAPPSRSRT-VGPSTCRKALWDGSLS-FLPFGASLLWFL--LWVLWDGAWLW----------------PRGLSRRGA 60
            PA PSRSR    P    K +WDGSL  ++  G   L++    +  WDG W W                 P GLSRR A
Sbjct  60  PAQPSRSRPQFAPPPGGKGVWDGSLGVYVIRGERDLYYRQRTYYRWDGGWFWSTSPQGPWTETDARGIPPGLSRRYA 136
```

ABC transporter protein (permease), ATP binding component [*Oceanicola granulosus* HTCC2516] ZP_01155864 (506 aa)

```
Tiga1    4  PAPPSRSRTVGPSTCRKALWDGSLSFLPFGASLLWFLLWVLWDGAWLWPRGLSRRGAGRGNAATLSLVSRLRRPVSEVS 82
            P  PS +   G +T  +++ DG +  L   ++L+  L  +   GA LW RG   R   R  A T+ L   + RPV +++
Sbjct  69  PQSPSAAMRAGIATVHQSIDDGVIPDLDVASNLM--LDRMAEPGAALWLRGRRMRAEARAIADTMQLDLDVSRPVRDLT 145
```

L-aspartate oxidase [*Bradyrhizobium japonicum* USDA 110] NP_769181 (536 aa)

```
Tiga1   60  AGRGNAATLSLVSRLRRPVSEVSGAVNKGSGLASGLRSH-VWKRGASSICV 109
            A RG A   ++V RLR  +S   G +  G GLA  + S    +R A+SI V
Sbjct 418  APRGGAPDAAVVKRLRATMSAHVGVIRHGDGLAEAVHSFAALERDATSIAV 468
```

Possible acetyltransferase [*Mycobacterium tuberculosis* H37Rv] CAB08300 (110aa)

```
Tiga1   34  ASLLWFLLWVLWDGA--------WLWPRGLSRRGAGRGNAATLS 69
            A  LWFL +  WDG         ++WPR   RRG  RG  +TL+
Sbjct  14  AMALWFLNFSTWDGVAGIYVEDLFVWPR-FRRRGLARGLLSTLA 56
```

CynX-related transport protein (cyanate permease), putative [*Deinococcus radiodurans* R1] AAF09845 (382 aa)

```
Tiga1   10 SRTVGPSTCRKALWDGSLSF---LPFGASLLWFLLWVLWDGAWLWPRGLSRRGAGRGNAATLSLVSRLRRP 77
           +R+ GP+    ++W    +    L  G   L F  W+ W    L  RGLS   AG    A LSL + ++ P
Sbjct 187 ARSAGPAVRGPSVWSNPATLPVTLYMGTQSLVFFTWLTWLARLLQDRGLSAEAAG----ALLSLGNLVQLP 253
```

Glycerol-3-phosphate regulon protein GlpG [*Sodalis glossinidius* str. 'morsitans'] BAE75602 (282 aa)

```
Tiag1   26 SLSFLPFGASLLWFLLWVLWDGAWLWPRGLSRRGAGRGNAATLSLVSRLRRPV--SEVSGAVNKG-SGLASGLRSHVWKRG 103
           S +FL F  SLL  L  V+W   W +  GL+ R  GR + A L ++S +   +  S  SG    G SG+   L  +VW  G
Sbjct 143 SHAFLHF--SLLHLLFNVVW---WWYLAGLTERYRGRASLAILFVLSAVVSGMVQSHFSGIFFGGLSGVVYALMGYVWWHG 218
```

Figure 9. Homology of Tiga1 with various proteins as determined by BLAST homology searching. Identical and homologous (+) amino acids are indicated. *TIGA1* ortholog exists only in primates but not in other organisms. Homologous protein of Tiga1 is found only in yeast and bacteria.

(Figure 9). The functions of these homologues are all somehow related to ion transport. That most of the Tiga-1 protein (78 of 120 amino acids) showed marked similarity (28% identical) to cyanate permease (a CynX-related transport protein) suggests that Tiga1 is involved in inorganic ion transport and metabolism. This is supported by the marked similarity of Tiga1 to the ABC transporter (permease). It is also notable that two of the Tiga1-homologue-bearing species identified to date are in symbiotic relationships; *Bradyrhizobium japonicum* is a nitrogen-fixing bacterium that develops a symbiotic relationship with the soybean plant (50), while *Sodalis glossinidius* is a maternally transmitted secondary endosymbiont that resides intracellularly in the tissues of the tsetse fly (51). Interestingly, most of the Tiga1 protein (78 of 120 amino acids) shows particularly extensive similarities (37% identical) to the glycerol-3-phosphate regulon protein GlpG of *S.glossinidius*. This suggests that the *TIGA1* gene may have entered the human genome after mice and humans separated. The existence of *TIGA1*-like genes in chimpanzees (Pan *troglodytes*) and

rhesus monkeys (*Macaca mulatta*) indicate that this event occurred before human beings diverged from monkeys. It is possible that the *TIGA-1* gene entered monkeys in Africa by a tsetse fly transposon. This possibility suggests that *TIGA-1* could serve as a molecular clock in the construction of a tree describing primate evolution; this tree could be useful for studying the evolution of human beings.

SUPPLEMENTARY DATA

Supplementary Data are available at NAR Online.

ACKNOWLEDGEMENTS

We thank members of RIKEN Cell bank (Tokyo, Japan) and Dr T. Kohno (National Cancer Center Research Institute, Tokyo, Japan) for the gifts of cancer cell lines. We also thank Dr S. Fujita for the anti-GFP antibody (J1) and Dr P. Hughes for critically reading the manuscript. This work was supported in part by the Innovation Plaza Osaka of the Japan Science and Technology Agency (JST), and by grants-in-aid for University and Society Collaboration, Scientific Research on Priority Areas 'Applied Genomics', Scientific Research (S), Exploratory Research, and the Science and Technology Incubation Program in Advanced Regions from the Ministry of Education, Culture, Sports, Science and Technology of Japan. This work was also supported by grants from the Osaka Cancer Society, the Yasuda Medical Research Foundation, the Welfide Medical Research Foundation, the Osaka Cancer Research Foundation and the Japanese Foundation for Multidisciplinary Treatment of Cancer. Funding to pay the Open Access publication charges for this article was provided by Scientific Research (S).

Conflict of interest statement. None declared.

REFERENCES

1. Pardee,A.B. (1974) A restriction point for control of normal animal cell proliferation. *Proc. Natl Acad. Sci. USA*, **71**, 1286–1290.
2. Zetterberg,A. and Larsson,O. (1985) Kinetic analysis of regulatory events in G1 leading to proliferation or quiescence of Swiss 3T3 cells. *Proc. Natl Acad. Sci. USA*, **82**, 5365–5369.
3. Cooper,S. (2003) Reappraisal of serum starvation, the restriction point, G0, and G1 phase arrest points. *FASEB J.*, **17**, 333–340.
4. Ren,S. and Rollins,B.J. (2004) Cyclin C/cdk3 promotes Rb-dependent G0 exit. *Cell*, **117**, 239–251.
5. Sage,J., Miller,A.L., Perez-Mancera,P.A., Wysocki,J.M. and Jacks,T. (2003) Acute mutation of retinoblastoma gene function is sufficient for cell cycle re-entry. *Nature*, **424**, 223–228.
6. Kamura,T., Hara,T., Matsumoto,M., Ishida,N., Okumura,F., Hatakeyama,S., Yoshida,M., Nakayama,K. and Nakayama,K.I. (2004) Cytoplasmic ubiquitin ligase KPC regulates proteolysis of p27(Kip1) at G1 phase. *Nature Cell Biol.*, **6**, 1229–1235.
7. Ogawa,H., Ishiguro,K., Gaubatz,S., Livingston,D.M. and Nakatani,Y. (2002) A complex with chromatin modifiers that occupies E2F- and Myc-responsive genes in G0 cells. *Science*, **296**, 1132–1136.
8. Schneider,C., King,R.M. and Philipson,L. (1988) Genes specifically expressed at growth arrest in mammalian cells. *Cell*, **54**, 787–793.
9. Cabrera,J.R., Sanchez-Pulido,L., Rojas,A.M., Valencia,A., Manes,S., Naranjo,J.R. and Mellstrom,B. (2006) GAS1 is related to the GDNF family receptors alpha and regulates ret signaling. *J. Biol. Chem.*, **281**, 14330–14339.
10. Benetti,R., Copetti,T., Dell'Orso,S., Melloni,E., Brancolini,C., Monte,M. and Schneider,C. (2005) The calpain system is involved in the constitutive regulation of β-catenin signaling functions. *J. Biol. Chem.*, **280**, 22070–22080.
11. Yoshioka,N., Inoue,H., Nakanishi,K., Oka,K., Yutsudo,M., Yamashita,A., Hakura,A. and Nojima,H. (2000) Isolation of transformation suppressor genes by cDNA subtraction: lumican suppresses transformation induced by v-src and v-K-ras. *J. Virol.*, **74**, 1008–1013.
12. Akagi,T., Shishido,T., Murata,K. and Hanafusa,H. (2000) v-Crk activates the phosphoinositide 3-kinase/AKT pathway in transformation. *Proc. Natl Acad. Sci. USA*, **97**, 7290–7295.
13. Nagamori,I., Yomgida,K., Adams,P., Sassone-Corsi,P. and Nojima,H. (2006) Transcription factors, cAMP-responsive element modulator (CREM) and Tisp40 act in concert in post-meiotic transcriptional regulation. *J. Biol. Chem.*, **281**, 15073–15081.
14. Toji,S., Yabuta,N., Hosomi,T., Nishihara,S., Kobayashi,T., Suzuki,S., Tamai,K. and Nojima,H. (2004) The centrosomal protein Lats2 is a phosphorylation target of Aurora-A kinase. *Genes Cells*, **9**, 383–397.
15. Kobori,M., Ikeda,Y., Nara,H., Kato,M., Kumegawa,M., Nojima,H. and Kawashima,H. (1998) Large scale isolation of osteoclast-specific genes by an improved method involving the preparation of a subtracted cDNA library. *Genes Cells*, **3**, 459–475.
16. Tsuruga,H., Yabuta,N., Hashizume,K., Ikeda,M., Endo,Y. and Nojima,H. (1997) Expression, nuclear localization and interaction of human MCM/P1 proteins . *Biochem. Biophys. Res. Commun.*, **236**, 118–125.
17. Fujii,T., Tamura,K., Masai,K., Tanaka,H., Nishimune,Y. and Nojima,H. (2002) Use of stepwise subtraction to comprehensively isolate mouse genes whose transcription is up-regulated during spermiogenesis. *EMBO Rep.*, **3**, 367–72.
18. Nelson,P.J. and Daniel,T.O. (2002) Emerging targets: molecular mechanisms of cell contact-mediated growth control. *Kidney Int.*, **61**, 99–105.
19. Smith,L.T., Lin,M., Brena,R.M., Lang,J.C., Schuller,D.E., Otterson,G.A., Morrison,C.D., Smiraglia,D.J. and Plass,C. (2006) Epigenetic regulation of the tumor suppressor gene TCF21 on 6q23-q24 in lung and head and neck cancer. *Proc. Natl Acad. Sci. USA*, **103**, 982–987.
20. Cui,S., Ross,A., Stallings,N., Parker,K.L., Capel,B. and Quaggin,S.E. (2004) Disrupted gonadogenesis and male-to-female sex reversal in Pod1 knockout mice. *Development*, **131**, 4095–4105.
21. Jeon,J.H., Lee,K.N., Hwang,C.Y., Kwon,K.S., You,K.H. and Choi,I. (2005) Tumor suppressor VDUP1 increases p27(kip1) stability by inhibiting JAB1. *Cancer Res.*, **65**, 4485–4489.
22. Yoshida,T., Nakamura,H., Masutani,H. and Yodoi,J. (2005) The involvement of thioredoxin and thioredoxin binding protein-2 on cellular proliferation and aging process. *Ann. N. Y. Acad. Sci.*, **1055**, 1–12.
23. Duncan,G., McCormick,C. and Tufaro,F. (2001) The link between heparan sulfate and hereditary bone disease: finding a function for the EXT family of putative tumor suppressor proteins. *J. Clin. Invest.*, **108**, 511–516.
24. Narayan,S., Thangasamy,T. and Balusu,R. (2005) Transforming growth factor-β receptor signaling in cancer. *Front. Biosci.*, **10**, 1135–1145.
25. Havens,C.G., Ho,A., Yoshioka,N. and Dowdy,S.F. (2006) Regulation of late G1/S phase transition and APC^{Cdh1} by Reactive Oxygen Species. *Mol. Cell. Biol.*, **26**, in press.
26. Li,N., Oberley,T.D., Oberley,L.W. and Zhong,W. (1998) Overexpression of manganese superoxide dismutase in DU145 human prostate carcinoma cells has multiple effects on cell phenotype. *Prostate*, **35**, 221–233.
27. Plymate,S.R., Haugk,K.H., Sprenger,C.C., Nelson,P.S., Tennant,M.K., Zhang,Y., Oberley,L.W., Zhong,W., Drivdahl,R. and Oberley,T.D. (2003) Increased manganese superoxide dismutase (SOD-2) is part of the mechanism for prostate tumor suppression by Mac25/insulin-like growth factor binding-protein-related protein-1. *Oncogene*, **22**, 1024–1034.
28. Galiatsatos,P. and Foulkes,W.D. (2006) Familial adenomatous polyposis. *Am. J. Gastroenterol.*, **101**, 385–398.
29. Ueno,K., Kumagai,T., Kijima,T., Kishimoto,T. and Hosoe,S. (1998) Cloning and tissue expression of cDNAs from chromosome 5q21–22 which is frequently deleted in advanced lung cancer. *Hum. Genet.*, **102**, 63–68.

30. No,D., Yao,T.P. and Evans,R.M. (1996) Ecdysone-inducible gene expression in mammalian cells and transgenic mice. *Proc. Natl Acad. Sci. USA*, **93**, 3346–3351.
31. Faderl,S., Gidel,C., Kantarjian,H.M., Manshouri,T., Keating,M. and Albitar,M. (2001) Loss of heterozygosity on chromosome 5 in adults with acute lymphoblastic leukemia. *Leuk. Res.*, **25**, 39–43.
32. Campisi,J., Morreo,G. and Pardee,A.B. (1984) Kinetics of G1 transit following brief starvation for serum factors. *Exp. Cell Res.*, **152**, 459–466.
33. Coller,H.A., Sang,L. and Roberts,J.M. (2006) A new description of cellular quiescence. *PLoS Biol.*, **4**, 329–349.
34. Jivotovskaya,A.V., Valasek,L., Hinnebusch,A.G. and Nielsen,K.H. (2006) Eukaryotic translation initiation factor 3 (eIF3) and eIF2 can promote mRNA binding to 40S subunits independently of eIF4G in yeast. *Mol. Cell Biol.*, **26**, 1355–1372.
35. Watanabe,H., Nonoguchi,K., Sakurai,T., Masuda,T., Itoh,K. and Fujita,J. (2005) A novel protein Depp, which is induced by progesterone in human endometrial stromal cells activates Elk-1 transcription factor. *Mol. Hum. Reprod.*, **11**, 471–476.
36. Basile,M., Lin,R., Kabbani,N., Karpa,K., Kilimann,M., Simpson,I. and Kester,M. (2006) Paralemmin interacts with D3 dopamine receptors: implications for membrane localization and cAMP signaling. *Arch. Biochem. Biophys.*, **446**, 60–68.
37. Lerner,L., Henriksen,M.A., Zhang,X. and Darnell,J.E., Jr (2003) STAT3-dependent enhanceosome assembly and disassembly: synergy with GR for full transcriptional increase of the alpha 2-macroglobulin gene. *Genes Dev.*, **17**, 2564–2577.
38. Chang,P., Coughlin,M. and Mitchison,T.J. (2005) Tankyrase-1 polymerization of poly(ADP-ribose) is required for spindle structure and function. *Nature Cell Biol.*, **7**, 1133–1139.
39. Jiang,H., Luo,S. and Li,H. (2005) Cdk5 activator-binding protein C53 regulates apoptosis induced by genotoxic stress via modulating the G2/M DNA damage checkpoint. *J. Biol. Chem.*, **280**, 20651–20659.
40. Banerjee,A.G., Bhattacharyya,I. and Vishwanatha,J.K. (2005) Identification of genes and molecular pathways involved in the progression of premalignant oral epithelia. *Mol. Cancer Ther.*, **4**, 865–875.
41. Denkert,C., Furstenberg,A., Daniel,P.T., Koch,I., Kobel,M., Weichert,W., Siegert,A. and Hauptmann,S. (2003) Induction of G0/G1 cell cycle arrest in ovarian carcinoma cells by the anti-inflammatory drug NS-398, but not by COX-2-specific RNA interference. *Oncogene*, **22**, 8653–8661.
42. Katsanis,N. (2004) The oligogenic properties of Bardet-Biedl syndrome. *Hum. Mol. Genet.*, **13**, 65–71.
43. Mak,H.Y., Nelson,L.S., Basson,M., Johnson,C.D. and Ruvkun,G. (2006) Polygenic control of *Caenorhabditis elegans* fat storage. *Nature Genet.*, **38**, 363–368.
44. Collin,G.B., Marshall,J.D., Ikeda,A., So,W.V., Russell-Eggitt,I., Maffei,P., Beck,S., Boerkoel,C.F., Sicolo,N., Martin,M. *et al.* (2002) Mutations in ALMS1 cause obesity, type 2 diabetes and neurosensory degeneration in Alstrom syndrome. *Nature Genet.*, **31**, 74–78.
45. Hearn,T., Renforth,G.L., Spalluto,C., Hanley,N.A., Piper,K., Brickwood,S., White,C., Connolly,V., Taylor,J.F., Russell-Eggitt,I. *et al.* (2002) Mutation of ALMS1, a large gene with a tandem repeat encoding 47 amino acids, causes Alstrom syndrome. *Nature Genet.*, **31**, 79–83.
46. Meyer-Lindenberg,A., Mervis,C.B., Sarpal,D., Koch,P., Steele,S., Kohn,P., Marenco,S., Morris,C.A., Das,S., Kippenhan,S. *et al.* (2005) Functional, structural, and metabolic abnormalities of the hippocampal formation in Williams syndrome. *J. Clin. Invest.*, **115**, 1888–1895.
47. Kobayashi,M., Nishita,M., Mishima,T., Ohashi,K. and Mizuno,K. (2006) MAPKAPK-2-mediated LIM-kinase activation is critical for VEGF-induced actin remodeling and cell migration. *EMBO J.*, **25**, 713–726.
48. Gorovoy,M., Niu,J., Bernard,O., Profirovic,J., Minshall,R., Neamu,R. and Voyno-Yasenetskaya,T. (2005) LIM kinase 1 coordinates microtubule stability and actin polymerization in human endothelial cells. *J. Biol. Chem.*, **280**, 26533–26542.
49. Takai,N., Ueda,T., Nishida,M., Nasu,K. and Narahara,H. (2006) Anticancer activity of MS-275, a novel histone deacetylase inhibitor, against human endometrial cancer cells. *Anticancer Res.*, **26**, 939–945.
50. Meakin,G.E., Jepson,B.J., Richardson,D.J., Bedmar,E.J. and Delgado,M.J. (2006) The role of *Bradyrhizobium japonicum* nitric oxide reductase in nitric oxide detoxification in soya bean root nodules. *Biochem. Soc. Trans.*, **34**, 195–196.
51. Dale,C., Jones,T. and Pontes,M. (2005) Degenerative evolution and functional diversification of type-III secretion systems in the insect endosymbiont *Sodalis glossinidius*. *Mol. Biol. Evol.*, **22**, 758–766.